Am J Transl Res 2020;12(9):5221-5236
www.ajtr.org /ISSN:1943-8141/AJTR0106964

Original Article

The restoration of Wnt/β-catenin signalling activity by a tuna backbone-derived peptide ameliorates hypoxia-induced cardiomyocyte injury

Le Zhang[1*], Minkai Cao[4*], Zhiwei Yu[2*], Siliang Xu[5*], Liang Ju[2], Jun Qian[2], Tianyu Li[2], Jianjuan Xu[4], Wei Qian[2], Jian Zhou[3], Zhengying Li[1]

Departments of [1]Neonatology, [2]Paediatrics, [3]Paediatric Laboratory, The Affiliated Wuxi Children's Hospital of Nanjing Medical University, Wuxi 214023, Jiangsu, China; [4]Department of Obstetrics, The Affiliated Wuxi Maternity and Child Health Care Hospital of Nanjing Medical University, Wuxi 214002, Jiangsu, China; [5]State Key Laboratory of Reproductive Medicine, Clinical Centre of Reproductive Medicine, First Affiliated Hospital, Nanjing Medical University, Nanjing 210029, China. [*]Equal contributors.

Received December 25, 2019; Accepted August 20, 2020; Epub September 15, 2020; Published September 30, 2020

Abstract: Myocardial infarction (MI) is a serious disease with high morbidity and mortality worldwide. Reducing myocardial reperfusion injury in MI patients remains a challenge. The generation of excessive reactive oxygen species (ROS) during reperfusion is known to be responsible for injury. A peptide from tuna backbone protein (APTBP) captured our attention due to its strong antioxidant activity. Here, we aimed to assess the function of APTBP in protecting against myocardial ischaemia-reperfusion (I/R) injury and to clarify the associated mechanism. Two in vitro models generated by hypoxia and cobalt chloride treatment were used to determine the effect of APTBP on cardiomyocytes under hypoxic stress. In vivo, a rat model of I/R was generated to evaluate APTBP functions. As a result, APTBP attenuated hypoxia- or cobalt chloride-induced injury to H9C2 cells and primary cardiomyocytes. Moreover, hypoxia-induced apoptosis, ROS generation and impaired mitochondrial function were also suppressed by APTBP administration. In vivo, tail vein injection of APTBP ameliorated pathological damage and mildly restored cardiac function. To clarify the mechanism, RNA-seq was performed and revealed that the Wnt signalling pathway may be associated with this mechanism. Rescue analysis showed that β-catenin knockdown diminished the protective effect of APTBP and that the expression of an ROS generator abolished the restoration of Wnt/β-catenin signalling induced by APTBP. Collectively, our findings suggest that APTBP reduces cardiomyocyte apoptosis and protects against myocardial ischaemia-reperfusion injury by scavenging ROS and subsequently restoring Wnt/β-catenin signalling.

Keywords: Myocardial infarction, APTBP, ROS, antioxidant

Introduction

Myocardial infarction (MI) is a leading cause of morbidity and mortality worldwide. Each year, approximately 800 thousand individuals in the United States suffer from a new MI [1, 2]. Despite significant advances in the medical management of MI, including primary percutaneous coronary intervention (PPCI), antiplatelet and antithrombotic therapies, and angioplasty, the prevalence of MI remains extremely high and constitutes a risk factor for heart failure.

The injury inflicted on the myocardium during acute MI mostly results from two detrimental processes, ischaemia and reperfusion, and is termed ischaemia-reperfusion (I/R) injury. The process of I/R is characterized by nutrient and oxygen deprivation that profoundly alters the outcome of a developing acute MI. Therefore, great efforts have been made to limit I/R injury.

Interestingly, therapeutic strategies applied solely at the onset of myocardial reperfusion have been shown to decrease MI size by 40-50% [3]. However, the mechanism responsible for reperfusion-induced injury has not yet been fully clarified. Paradoxically, reperfusion with oxygen-rich blood further damages the ischaemic myo-

cardium. Furthermore, a burst of reactive oxygen species (ROS) generation has been well described during the first few moments of reperfusion. Experimental studies have supported the notion of oxidative stress-induced reperfusion injury when oxygen is reintroduced to ischaemic tissue [4]. Previous studies have documented that the generation of ROS is dramatically elevated by more than three-fold in animal hearts that underwent ischaemia/reperfusion compared to that of normal hearts [5]. ROS modulate some important pathways, including apoptosis, energy metabolism, the inflammatory response, and survival/stress responses [6]. Excess ROS accumulation is understood to represent a common pathogenic mechanism of the progression of I/R.

Given the important role of ROS in I/R injury, strategies aimed at eliminating excessive ROS may be effective therapeutic approaches to reducing damage associated with I/R. Some evidence has suggested that restricting I/R-induced ROS accumulation and myocardial apoptosis greatly benefits patients who suffer from MI [7]. In addition, a few antioxidants have been determined to have cardioprotective effects by countering oxidative stress [8, 9].

Recently, a novel peptide purified from the hydrolysates of tuna backbone protein (APTBP) has been identified to have strong antioxidant activity [10, 11]. In vitro experiments have revealed the antioxidant effects of APTBP in inhibiting lipid peroxidation and scavenging free radicals. This observation prompted us to consider whether APTBP may be an effective molecule for protecting against I/R-induced myocardial injury.

Therefore, in the present study, we investigated the effect of APTBP in myocardial ischaemia-reperfusion injury. We first explored the function of APTBP in a hypoxic cardiomyocyte model and in a rat model of I/R. Furthermore, through transcriptome analysis, we preliminarily clarified the mechanism underlying the cardioprotective effect of APTBP.

Materials and methods

Cell culture and hypoxic stimulation

The embryonic heart-derived H9C2 cell line was obtained from the Chinese Academy of Science (Shanghai, China). H9C2 cells were cultured in Dulbecco's modified Eagle's medium (DMEM) (Thermo Fisher Scientific, Waltham, MA, USA) supplemented with 10% foetal bovine serum (FBS), 100 U/ml penicillin (Wisent, Canada) and 100 μg/ml streptomycin (Wisent, Canada) in a humidified incubator with 5% CO_2 at 37°C.

For primary ventricular myocyte isolation, 2-day-old Sprague-Dawley rats were dissected, and the ventricles were minced and digested with collagenase (0.4 mg/ml, Sigma Aldrich) and pancreatin (0.6 mg/ml) in 116 mM NaCl, 20 mM HEPES (pH 7.35), 5.6 mM glucose, 0.8 mM NaH_2PO_4, 5.4 mM KCl, and 0.8 mM $MgSO_4$. The cells were recovered by centrifugation (5 min, 100× g), resuspended in DMEM containing 15% M199 and 15% FCS and plated on 10-cm dishes precoated with 1% gelatine (37°C, 30 min) to remove non-myocytes. The non-adherent cardiomyocytes were isolated and plated on gelatine-coated six-well dishes at a density of 2×10^5 cells per well.

To generate the hypoxia model, H9C2 cells and primary ventricular cells were cultured in dishes with DMEM supplemented with 10% serum and divided into the experimental group and the control group. The cells in the experimental group were pre-treated with peptide for 1 h and then cultured in serum- and glucose-free medium. The cells were then anaerobically cultured using the AnaeroPack system (Mitsubishi Gas Chemical Co., Inc., Tokyo, Japan) for 12 h and reoxygenated for 3 h at 37°C (for the in vitro hypoxia time course experiment, the reperfusion period was held constant at 3 h). The cells in the control group were cultured in normal medium. For cobalt chloride ($CoCl_2$) treatment, 800 μM $CoCl_2$ was added to the culture supernatant of H9C2 cells, and the cells were cultured for 18 h with 5% CO_2 at 37°C after pre-administration of the peptide.

A trypan blue dye exclusion assay was performed to detect cell survival. To examine the cell death rate, the cells were collected and stained using a trypan blue staining cell viability assay kit (Beyotime, China) according to the manufacturer's protocol. The blue-stained cells were regarded as dead cells, and the death rate was calculated by the following formula: dead cells/total cells ×100%.

Determination of the lactate dehydrogenase (LDH) level

The level of lactate dehydrogenase released into the culture supernatant and in rat serum was examined by an LDH release assay kit (Beyotime, China) according to the manufacturer's instructions.

Peptide synthesis

The peptides used in the study were synthesized and purified by Science Peptide (Shanghai, China). APTBP (VKAGFAWTANQQLS) and scramble APTBP (ANVQSAAGWLQTFK) contained 13 amino acids (GRKKRRQRRRPPQ) constituting a cell-penetrating peptide (CPP) derived from the HIV-1 Tat region (48-60). The peptides were dissolved in water at a concentration of 10 mM and stored in a -80°C freezer.

TUNEL staining assay

For the terminal deoxytransferase-mediated dUTP-biotin nick end labelling (TUNEL) assay, the cells were washed with phosphate-buffered saline (PBS) three times and immobilized with 4% paraformaldehyde. Apoptotic cells were visualized with TUNEL staining according to the manufacturer's instructions (Beyotime, China). The percentage of TUNEL-positive cells was determined by calculating the ratio of TUNEL fluorescence intensity to the DAPI fluorescence intensity, and the fluorescence intensity was determined using ImageJ software 1.26 (Wayne Rasband, National Institutes of Health, Bethesda, MD, USA).

Determination of oxygen consumption

After exposure to hypoxia, H9C2 cells were evaluated for oxygen consumption using a Seahorse extracellular flux analyser (Seahorse Biosciences, Billerica, CA, USA). The proportion of oxygen consumption due to ATP turnover, the maximal rate of respiration and the amount of proton leak were determined by injecting 1 μM oligomycin A, 1 μM FCCP and 10 μM antimycin A at the indicated times.

In vivo experiment

The animal study protocol was in accordance with the Care and Use of Animals published by the Institutional Animal Ethical Committee. Male Sprague-Dawley rats (8 weeks old) were randomly assigned to three groups: the sham-operated group (n=6), the I/R group (n=6), and the peptide-treated I/R group (n=6×3). All of the rats were injected with APTBP or an equal volume of scramble APTBP (the peptides were all dissolved in saline) *via* the caudal vein 30 min before the I/R procedure. The rats were anaesthetized with chloral hydrate (400 mg/kg) *via* intraperitoneal injection. A thoracotomy was performed, and myocardial I/R was induced by ligating the left anterior descending (LAD) coronary artery with a 6-0 silk suture for 40 min before 24 h of reperfusion. The sham operation was conducted using the entire surgical protocol described above without LAD ligation and release. Then, the hearts were harvested for paraffin embedding and sectioning and were stained with haematoxylin & eosin (H&E) or Masson's trichrome. For TTC staining, the heart was frozen at -20°C for 1 h, cut into slices perpendicular to the apex-base axis, incubated in 1.0% TTC for 20 min at 37°C, and immersed in 10% formalin overnight. The scoring criteria for the myocardial injury histoscore were previously described [12]. Briefly, the pathology was scored as 0 (nil, no myocardial injury), 1 (minimum, minimal myocardial injury), 2 (mild, visibly disorganized myocardial fibres), 3 (moderate, obviously disorganized myocardial fibres), or 4 (severe, severely disorganized myocardial fibres and focal destruction by neutrophil infiltration). The tissue from the MI area was lysed and evaluated for caspase-3 activity using a caspase-3 activity kit (Beyotime Institute of Biotechnology, Haimen, China) according to the manufacturer's instructions.

The mice underwent 40 min of ischaemia and 24 h of reperfusion and were evaluated for cardiac function through transthoracic echocardiography using a Vevo 2100 system (Visual Sonics, Toronto, Canada). Two-dimensional-guided M-mode echocardiography was used to determine the left ventricular chamber volume at systole and diastole and contractile parameters, such as the left ventricular end-diastolic dimension (LVEDD), the left ventricular end-systolic dimension (LVESD), the left ventricular end-diastolic volume (LVEDV), and the left ventricular end-systolic volume (LVESV). The left ventricular fractional shortening (LVFS) was calculated as follows: FS (%)=(LVEDD-LVESD)/LVEDD×100. The ejection fraction (EF) was then derived as EF (%)=(EDV-ESV)/EDV×100.

Western blot analysis

Protein was extracted from the cells with RIPA lysis buffer containing 1% PMSF and quantified using a BCA protein assay kit (23229; Thermo Fisher Scientific). A total of 30 μg of protein was mixed with 1× SDS sample loading buffer and separated on a 10% SDS-PAGE gel. Anti-caspase-3 (#9665) (1:2000), anti-β-catenin (#8480) (1:1000), anti-cyclin D1 (#2922) (1:2000), and anti-β-actin (#3700) (1:5000) were purchased from Cell Signaling Technology (Danvers, MA, USA). Anti-GSK3β (ab93926) (1:2000), anti-APC (ab40778) (1:1000) and anti-Axin2 (ab32197) (1:1000) antibodies were purchased from Abcam (Cambridge, MA, USA). The immunoreactive bands were detected by a FluorChem M system (ProteinSimple, San Jose, CA, USA).

Knockdown of β-catenin

Twenty thousand H9c2 cells were plated in 6-well plates, and 24 h later, when the cells reached approximately 60% confluence, 100 pmol of siRNA was transfected into the cells using Lipofectamine 2000 (Thermo Fisher Scientific, Waltham, MA, USA). Forty-eight hours post-transfection, the cells were used for peptide treatment or hypoxic stimulation. The siRNAs used in this study were purchased from Santa Cruz Biotechnology (Santa Cruz, CA, USA).

Transcriptomic analysis

The cells that underwent hypoxia were treated with APTBP (50 μM) or left untreated. Then, total RNA was isolated as previously described and submitted for transcriptome analysis using Illumina HiSeq. A TruSeq RNA sample prep kit v2 (Illumina) was used to prepare the cDNA libraries according to the manufacturer's instructions. The size distribution of the final product was assessed using a Bioanalyzer DNA High Sensitivity Kit (Agilent Technologies). Each library was loaded into one lane of an Illumina HiSeq 2500 for 2×150 bp paired-end (PE) sequencing.

Following on-board cluster generation on a Rapid Run paired-end flow cell, the libraries subsequently underwent 150 cycle sequencing (v3 sequencing kit) according to the manufacturer's instructions (HiSeq 2500, Illumina). The differentially regulated genes were analysed using ClueGO + Cluepedia.

ROS determination and generation

For intracellular ROS assessment, ROS levels were determined by a reactive oxygen species assay kit (Beyotime, China) according to the manufacturer's instructions. Briefly, after being cultured in serum-free DMEM containing 0.1% DCFH-DA at 37°C for 20 min, the cells were washed with serum-free DMEM three times and photographed using a laser scanning confocal microscope. The ROS fluorescence intensity was assessed using ImageJ software and normalized to that of the control.

For the DPPH (2,2-diphenyl-1-picrylhydrazyl) assay, the procedure was performed according to a previous study [13]. Briefly, 1 mg DPPH was dissolved in 24 ml of ethyl alcohol, and different concentrations of APTBP were added to the DPPH solution to evaluate the radical scavenging ratio by measuring the absorbance at 519 nm.

For mitochondrial ROS determination, H9c2 cells were stained with CellROX Deep Red Reagent (Thermo Fisher, USA) and MitoTracker™ Green (Thermo Fisher, USA) for 40 min and then washed with PBS 3 times. The fluorescent images were photographed using a Leica fluorescence stereomicroscope model MZ FL III (Leica, Germany).

For ROS generation, D-galactose (0.5 mM) and galactose oxidase (GAO) (0.015 U/ml) were used to generate exogenous H_2O_2 as previously described [12]. The reagents were purchased from Sigma Aldrich (St. Louis, MO, USA).

Statistical analysis

Statistical analyses were performed using SPSS 13.0 software. All experiments were repeated at least three times with similar results, and Student's *t*-test or one-way ANOVA followed by a post hoc Tukey test was used to assess significance.

Results

The basic characteristics of APTBP

We first identified the basic characteristics of APTBP using the ProtParam tool (https://web.

Table 1. Characterization of APTBP

Formula	MW	pI	Half-life (h)	Instability index	GRAVY
$C_{69}H_{105}N_{19}O_{20}$	1520.7	8.72	100	4.86	-0.071

GRAVY: Grand average of hydropathicity.

expasy.org/protparam/) and Helical Wheel Projections software (http://rzlab.ucr.edu/scripts/wheel/wheel.cgi). Analyses with the ProtParam tool revealed that the protein had a theoretical half-life of up to 100 h, demonstrating the stability of APTBP (**Table 1**). Based on helical wheel projections, APTBP appeared to have a significant amphipathic character, with three distinct hydrophobic residues (F5, W7, and L13), along with three distinct hydrophilic residues (N10, Q11, and Q12) (the most hydrophobic residues are coded green, and the hydrophilic residues are coded red) (**Figure 1A**). Considering that the cell membrane is a barrier for peptides to enter the cell and exert their functions, we chemically synthesized APTBP with a cell-penetrating peptide (CPP: GRKKRRQRRRPPQ) derived from HIV-1 Tat (48-60) attached to the N terminus. To determine the stability and cell-penetrating ability of the synthesized APTBP, embryonic heart-derived H9C2 cells were treated with FITC-labelled APTBP (10 μM), and the fluorescence was monitored at different time points. APTBP penetrated the cell membrane readily and resided intracellularly, including in the nucleus, after 3 h. The fluorescence intensity remained relatively constant at 9 h, but the majority of the signal had declined by 18 h (**Figure 1B**). These results demonstrate that APTBP is able to easily penetrate the cell and displays sufficient intracellular stability, which provides support for subsequent in vitro and in vivo studies.

APTBP protected cardiomyocytes from hypoxia-induced injury

To investigate whether APTBP is able to protect cardiomyocytes against hypoxic stress, we determined the impact of APTBP administration on hypoxia-induced damage to H9C2 cells. Hypoxia caused more than half of the H9C2 cells to become round and float, indicating cellular death. Although the scramble peptide and low doses of APTBP (10 μM) exhibited no significant protective effects, doses of 20 μM, 50 μM, and 100 μM markedly decreased cardiomyocyte death in a dose-dependent manner, as well as the level of LDH released into the cell culture supernatant (**Figure 2A-C**). Because 50 μM peptide showed a marked effect similar to that of the 100 μM dose, we selected 10, 20, and 50 μM APTBP for subsequent studies. Then, we assessed alterations in the cell death rate at different time points and found that APTBP (50 μM) caused a significant reduction in the death rate after 6-12 h of hypoxia treatment (**Figure 2D**).

To confirm the protective effect of APTBP on hypoxia-induced injury, we used $CoCl_2$, a compound that rapidly increases intracellular ROS levels, to chemically mimic hypoxia. Consistently, APTBP (50 μM) notably attenuated $CoCl_2$-induced H9C2 cell death and decreased the death rate from approximately 0.8 to 0.4 (**Figure 2E**, **2F**). APTBP also reduced hypoxia-induced primary myocardial cell death (**Figure 2G**). Taken together, these results demonstrate that APTBP possesses a strong protective effect against hypoxic stress and exhibits a favourable protective effect in cardiomyocytes.

APTBP inhibited hypoxia-induced apoptosis

Limited ischaemia is understood to mainly induce apoptosis in cardiomyocytes. Therefore, Western blot analysis of cleaved caspase-3 expression was conducted to examine the level of apoptosis in H9C2 cells. We observed a dramatic decrease in the level of cleaved caspase-3 after APTBP treatment. Compared to the hypoxia group, the group treated with 20 μM APTBP exhibited an almost 50% reduction in the expression of cleaved caspase-3 (**Figure 3A**, **3B**).

We next used a TUNEL assay to measure apoptotic cells and observed that APTBP (50 μM) significantly reduced the number of TUNEL-positive cells, and the proportion decreased from approximately 70% to 40% (**Figure 3C**, **3D**). These results indicate that APTBP inhibits apoptosis and exhibits a protective effect in cardiomyocytes exposed to hypoxia.

APTBP reduced ROS accumulation and restored mitochondrial function

A previous study showed that APTBP possesses the ability to engage in direct free radical scavenging and exhibits antioxidant activity [14]. Given that hypoxia commonly increases

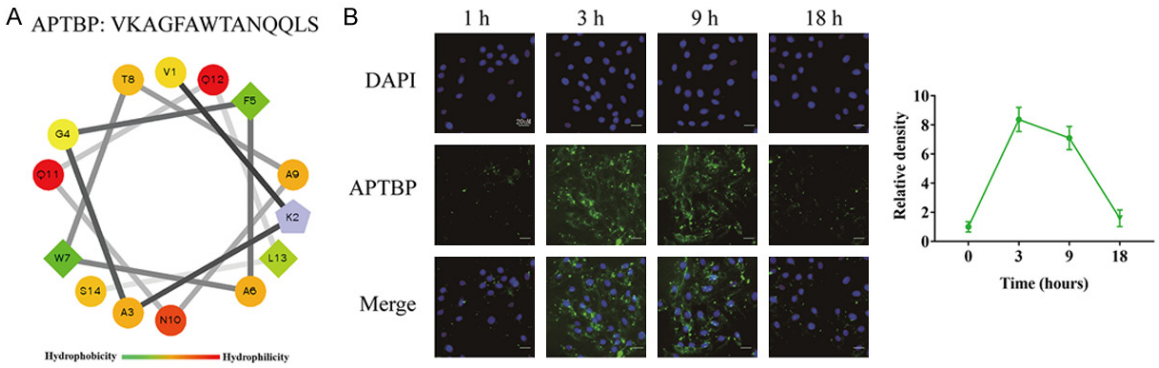

Figure 1. The basic characteristics of APTBP. A. Helical wheel representations of APTBP. Numbers indicate the location of these motifs in the peptide APTBP. The structure presents hydrophilic residues as circles, hydrophobic residues as diamonds, potentially negatively charged residues as triangles, and potentially positively charged residues as pentagons. Hydrophobicity is colour coded as well: the most hydrophobic residue is green, and the amount of green is decreased proportionally to the hydrophobicity, with zero hydrophobicity coded as yellow. Hydrophilic residues are coded red, with pure red being the most hydrophilic (uncharged) residue, and the amount of red decreasing proportionally to the hydrophilicity. The potentially charged residues are light blue. B. Fluorescent images of the intracellular distribution of FITC-labelled APTBP and the relative density. As described, after the peptide was added, the fluorescence was monitored at 1, 3, 9, and 18 h. Three replicate experiments were conducted and analysed. Scale bar: 20 μm. H9c2 cells were treated with APTBP (10 μM) for the indicated time and photographed under a fluorescence microscope.

cytotoxic ROS accumulation, which always leads to mitochondrial dysregulation and cell damage, we next assessed the intracellular ROS levels after APTBP administration by fluorescence microscopy using DCFH-DA. The results showed that the levels of intracellular ROS were increased dramatically under hypoxic stress, and APTBP potently restricted ROS accumulation, while the scramble peptide had no effect (**Figure 4A**, **4B**).

Mitochondria are understood to play a crucial role in maintaining the normal function of cardiomyocytes. Accordingly, we validated mitochondrial function after treatment with APTBP by measuring the oxygen consumption rate using a Seahorse extracellular flux analyser. We observed that hypoxia markedly impaired not only basal respiration but also maximal respiration in cardiomyocytes (**Figure 4C**). The administration of APTBP partly restored the rate of oxygen consumption, suggesting a protective effect on mitochondria (**Figure 4C**). Taken together, these results suggest that APTBP eliminates ROS accumulation and protects mitochondria against hypoxic stress, potentially maintaining normal cardiomyocyte function.

APTBP attenuated cardiomyocyte injury caused by ischaemia-reperfusion in vivo

We next examined whether APTBP exhibits a cardioprotective effect in vivo similar to that observed in vitro. To address this, an I/R model was generated in male SD rats by LAD ligation for 40 min followed by 3 h of reperfusion. **Figure 5A** shows a schematic of the procedure used to generate the animal model. The echocardiography results showed that 20 mg/kg APTBP mildly restored myocardial function, such as the EF (ejection fraction) and FS (fractional shortening) indices, the HW/BW (heart weight/body weight) ratio, LV (left ventricular) mass and cardiomyocyte CSA (cross-sectional area) (**Figures 5B**, S1). TTC, HE and Masson staining showed severely disorganized myocardial fibres and focal destruction by neutrophil infiltration in the hearts that were exposed to I/R (**Figure 5C-E**). APTBP (20 mg/kg) reduced the ischaemic area, restored the relative integrated organization of myocardial fibres, and improved myocardial fibrosis (**Figure 5C-E**). In addition, the ROS level in primary cardiomyocytes was also reduced upon APTBP administration (Figure S2). Moreover, the serum level of LDH, which serves as a sensitive marker of cardiomyocyte injury, decreased in response to 20 mg/kg APTBP treatment (**Figure 5F**). We then measured the activity of caspase-3, the activation of which reflects the level of apoptosis. The results showed that the mice exposed to 20 mg/kg APTBP exhibited decreased caspase-3 activity compared with that of I/R mice, indicating a reduced apoptosis level (**Figure 5G**). These observations suggest a mild cardio-

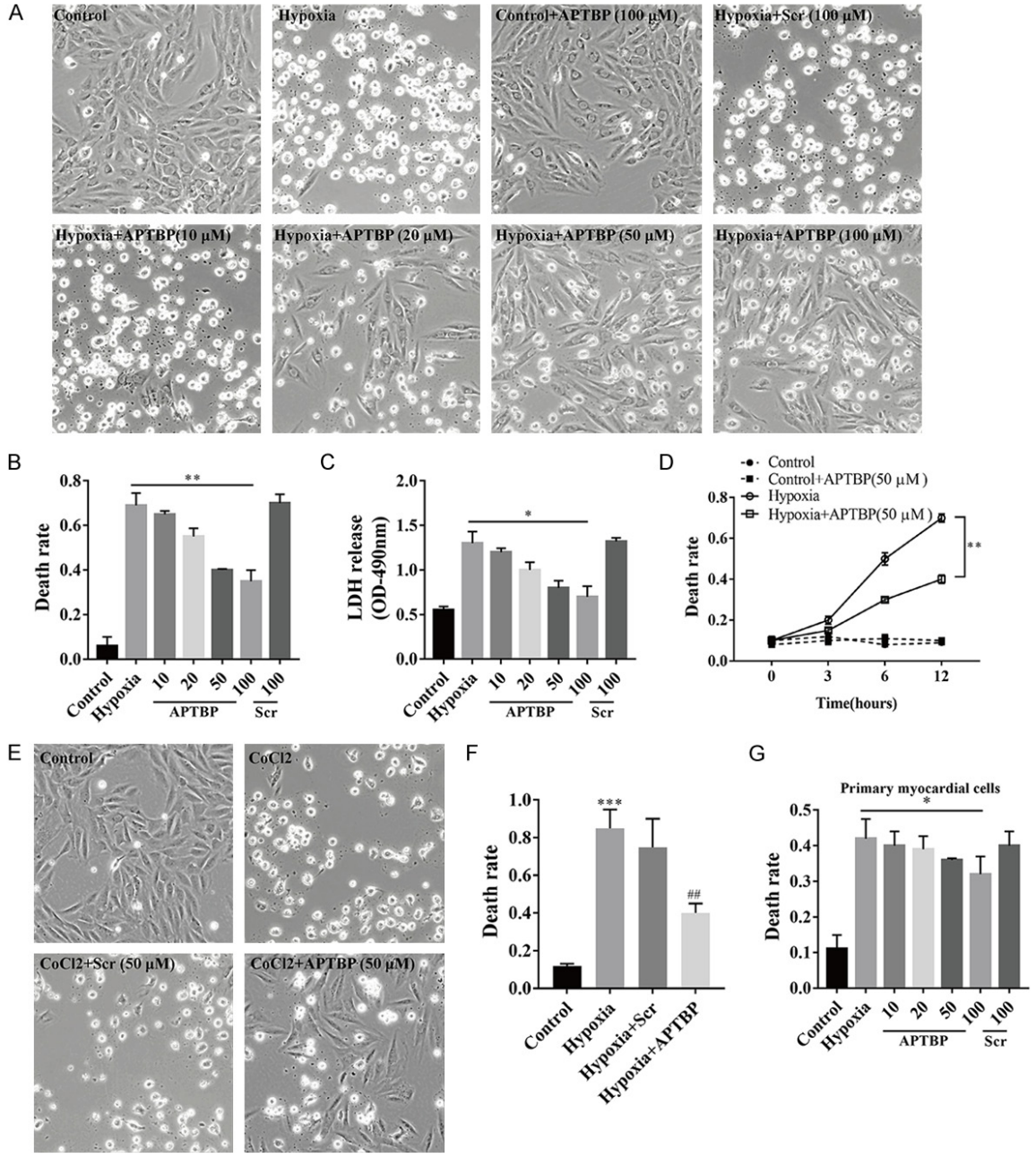

Figure 2. APTBP protected cardiomyocytes from hypoxia-induced injury. H9c2 cells were pre-treated with different doses of peptides for 1 h, then treated as indicated and analysed after 12 h of hypoxia and 3 h of reoxygenation. A. Photographs obtained using phase-contrast microscopy; scale bar: 20 μm. B. The death rate measurement by trypan blue dye staining. C. The LDH level in the culture supernatant. D. The death rate of H9c2 cells treated as indicated for different hypoxia times (the reoxygenation time remained the same). One-way ANOVA was used to compare the differences between groups. **P<0.001. E. H9c2 cells were pre-treated with APTBP (50 μM) for 1 h and then treated with 800 μM $CoCl_2$ for 18 h and photographed using phase-contrast microscopy; scale bar: 20 μm. F. Death rate measurement by trypan blue dye staining. Student's *t*-test was used to compare the differences between the control and hypoxia groups (***P<0.001) and the hypoxia and APTBP treatment groups (##P<0.01). G. Primary myocardial cells were pre-treated with different doses of peptides for 1 h and then challenged with hypoxia (12 h)/reoxygenation (3 h), and the death rates were determined. Scr denotes the scramble peptide of APTBP. The death rate was calculated *via* trypan blue analysis. **P<0.01, *P<0.05. One-way ANOVA was used to compare differences between groups. The data are shown as the means ± SD. All experiments were repeated three times with similar results.

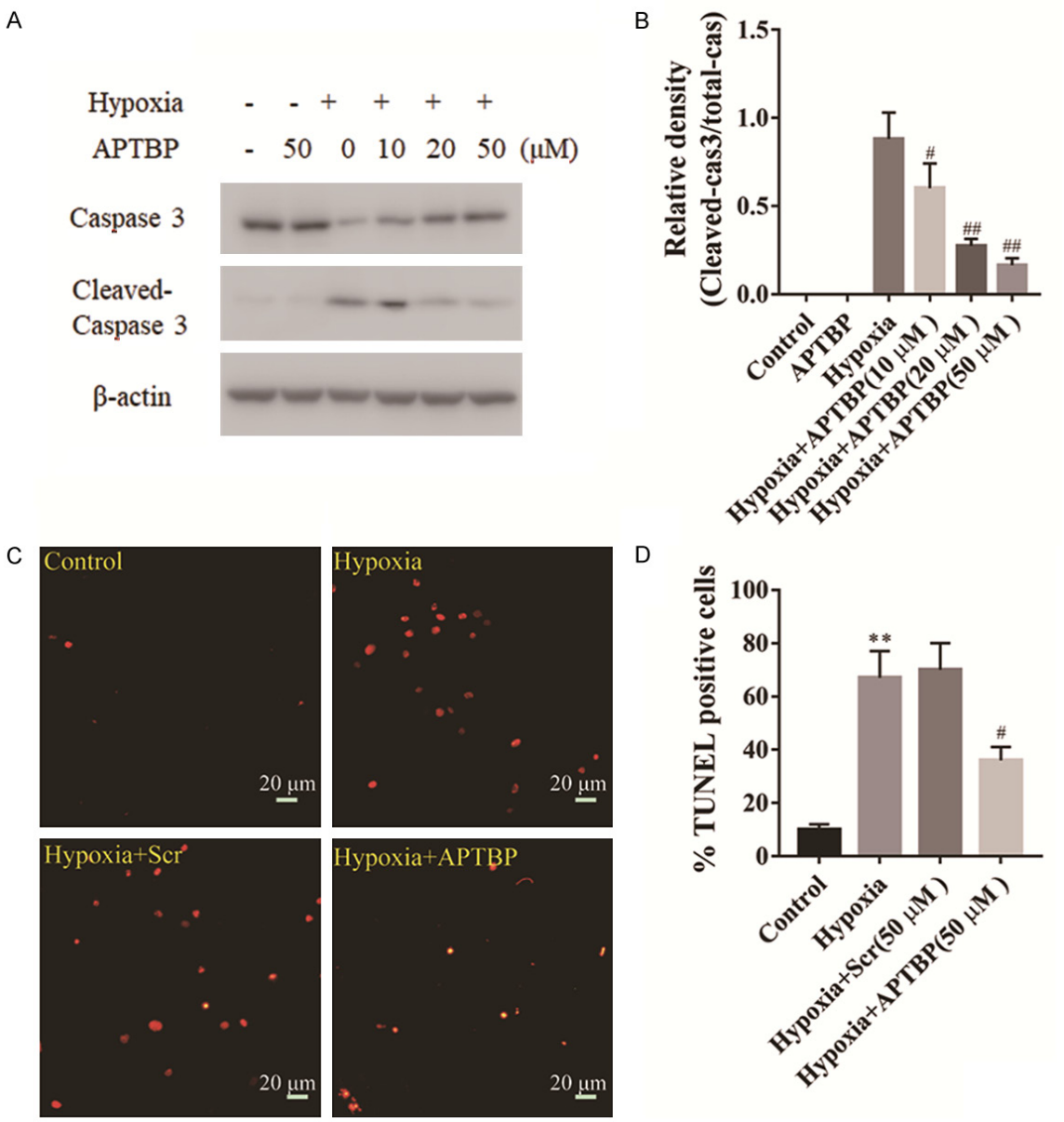

Figure 3. APTBP inhibited hypoxia-induced apoptosis. A. After 1 h of pre-treatment with peptide and hypoxia (12 h)/reoxygenation (3 h) challenge, H9c2 cells were harvested and subjected to Western blot analysis of cleaved caspase-3. B. The relative density was calculated by dividing the cleaved caspase 3 level by the total caspase 3 level. Three replicate experiments were conducted and analysed. C. Fluorescent images of TUNEL staining; scale bar: 20 μm, D. The proportion of TUNEL-positive cells. $^{**}P<0.01$ versus the control group. $^{\#}P<0.05$, $^{\#\#}P<0.01$ versus the hypoxia group. Student's *t*-test was used to compare differences between groups. The data are shown as the means ± SD. All experiments were repeated four times with similar results.

protective effect of APTBP on I/R-induced myocardial injury in vivo.

Transcriptome analysis of H9C2 cells treated with APTBP

Based on the nuclear distribution of APTBP (**Figure 1B**), we examined whether APTBP also functions by regulating the transcription of certain genes. Hence, global transcriptome analysis was used to analyse the alterations in gene expression after APTBP treatment to clarify the mechanism underlying the cardioprotective effect of APTBP. A total of 11512 genes were detected, 1485 of which were significantly differentially expressed (P<0.05) (**Figure 6A**). To evaluate the potential signalling pathways involved in APTBP-mediated amelioration of

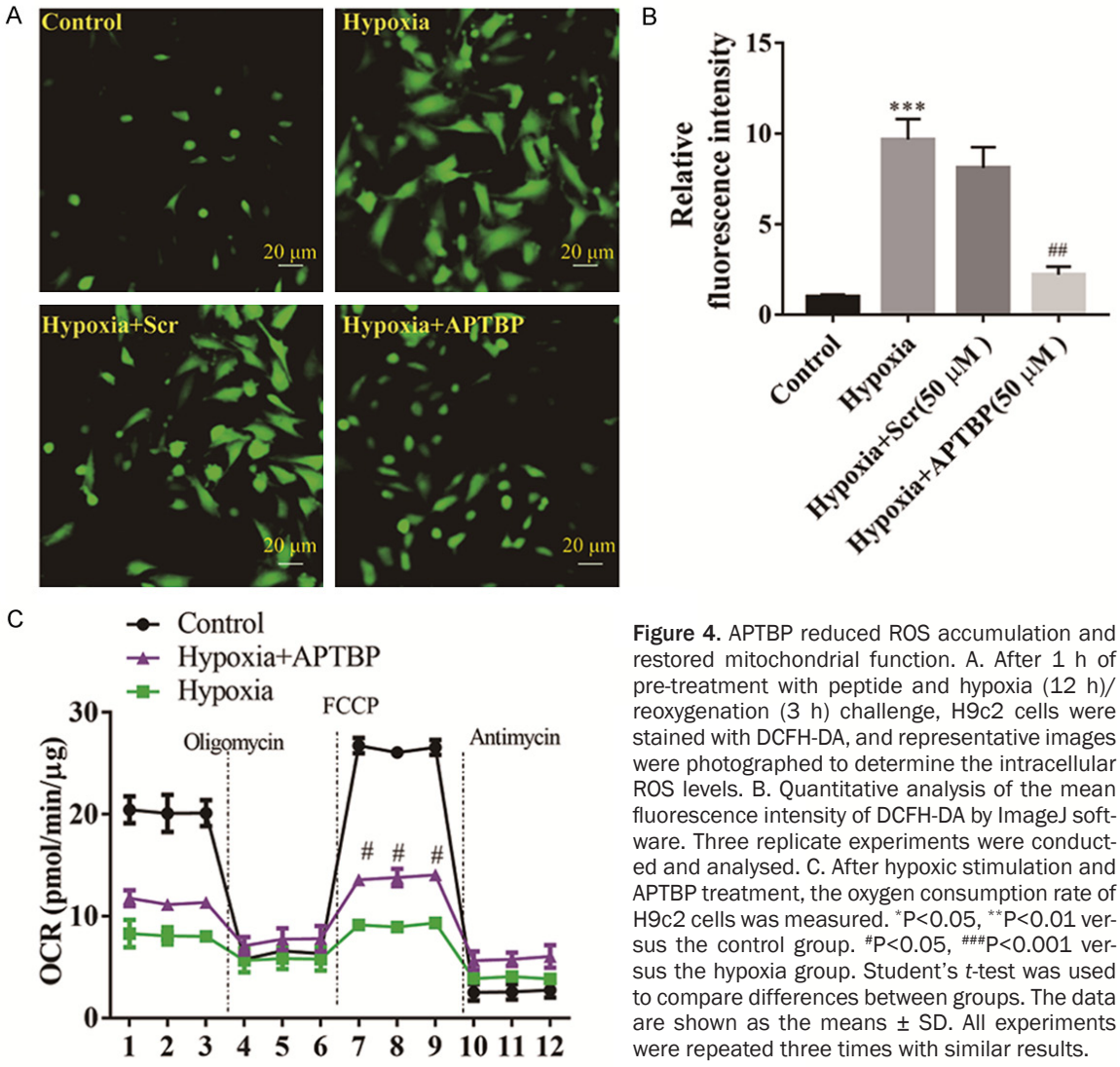

Figure 4. APTBP reduced ROS accumulation and restored mitochondrial function. A. After 1 h of pre-treatment with peptide and hypoxia (12 h)/reoxygenation (3 h) challenge, H9c2 cells were stained with DCFH-DA, and representative images were photographed to determine the intracellular ROS levels. B. Quantitative analysis of the mean fluorescence intensity of DCFH-DA by ImageJ software. Three replicate experiments were conducted and analysed. C. After hypoxic stimulation and APTBP treatment, the oxygen consumption rate of H9c2 cells was measured. $^{*}P<0.05$, $^{**}P<0.01$ versus the control group. $^{\#}P<0.05$, $^{\#\#\#}P<0.001$ versus the hypoxia group. Student's *t*-test was used to compare differences between groups. The data are shown as the means ± SD. All experiments were repeated three times with similar results.

hypoxic injury, the differentially expressed genes were subjected to KEGG pathway analysis. The results demonstrated a significant enrichment in signalling pathways that regulate the pluripotency of stem cells (rno04550), the Wnt signalling pathway (rno04310), pathways involved in cancer (rno05200), the transforming growth factor beta (TGF-beta) signalling pathway (rno04350), and the Hippo signalling pathway (rno04390) (**Figure 6B**, **6C**). These observations suggest that these signalling pathways are implicated in the cardioprotective mechanism of APTBP.

APTBP restored the activity of Wnt/β-catenin in cells injured by hypoxia

Among the enriched pathways identified by KEGG pathway analysis, the Hippo and the signalling pathways captured our attention. The Hippo pathway is known to control the balance between proliferation, differentiation and apoptosis in cells [15]. As key downstream effectors of the Hippo pathway, YAP (yes-associated protein)/TAZ (transcriptional coactivator with PDZ-binding motif) are dephosphorylated and translocate to the nucleus when the Hippo pathway is not activated and interact mainly with TEAD family transcription factors to initiate the expression of genes that promote cell proliferation and inhibit apoptosis [16, 17]. Indeed, hypoxia induced a strong decrease in YAP phosphorylation, suggesting inhibition of the Hippo signalling pathway under hypoxic stress conditions. However, no significant difference in the level of phosphorylated YAP was detected after APTBP administration (**Figure 7A**). These

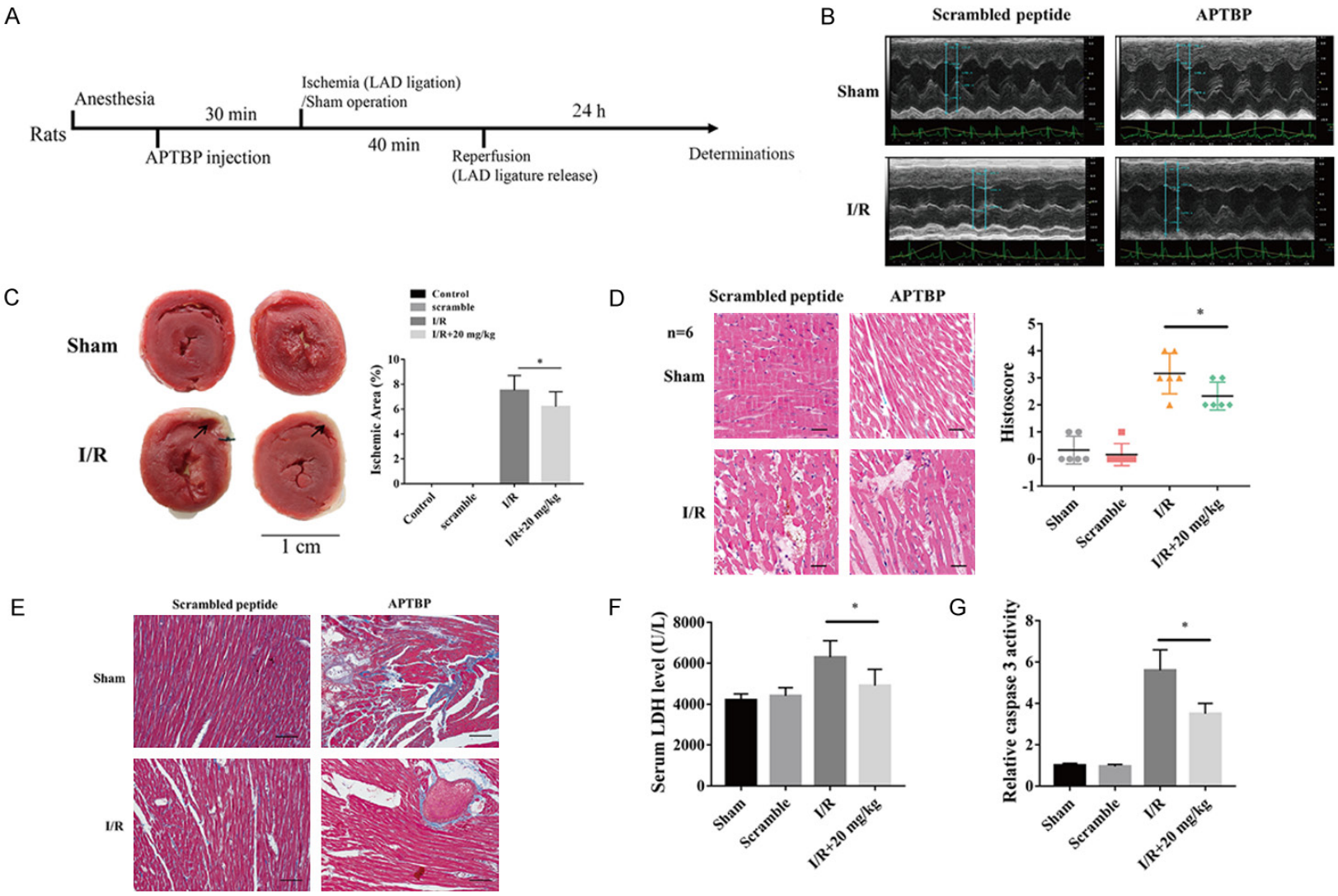

Figure 5. APTBP attenuated cardiomyocyte injury caused by ischaemia-reperfusion in vivo. A. Outline of the experimental procedure for the rat I/R model. After the procedure, rats were subjected to subsequent analysis. B. Echocardiography. C. Rat hearts were extracted for TTC staining and ischaemic area measurement. Student's *t*-test was used to compare differences between groups, *P<0.05. D. Left panel, Representative histopathological analysis of rat hearts after the indicated treatments; scale bar: 50 μm. Right panel, the extent of myocardial lesions was evaluated by the histoscore. The score standard was described in the methods section. E. Masson staining; scale bar: 100 μm. F. After treatment, the serum LDH level of the rats was determined. There were six rats per group. G. Cardiac muscle tissue was minced and lysed for caspase 3 activity measurement, and three replicate experiments were conducted and analysed. *P<0.05. Student's *t*-test was used to compare differences between groups. The data are shown as the means ± SD. Each group contained 6 rats.

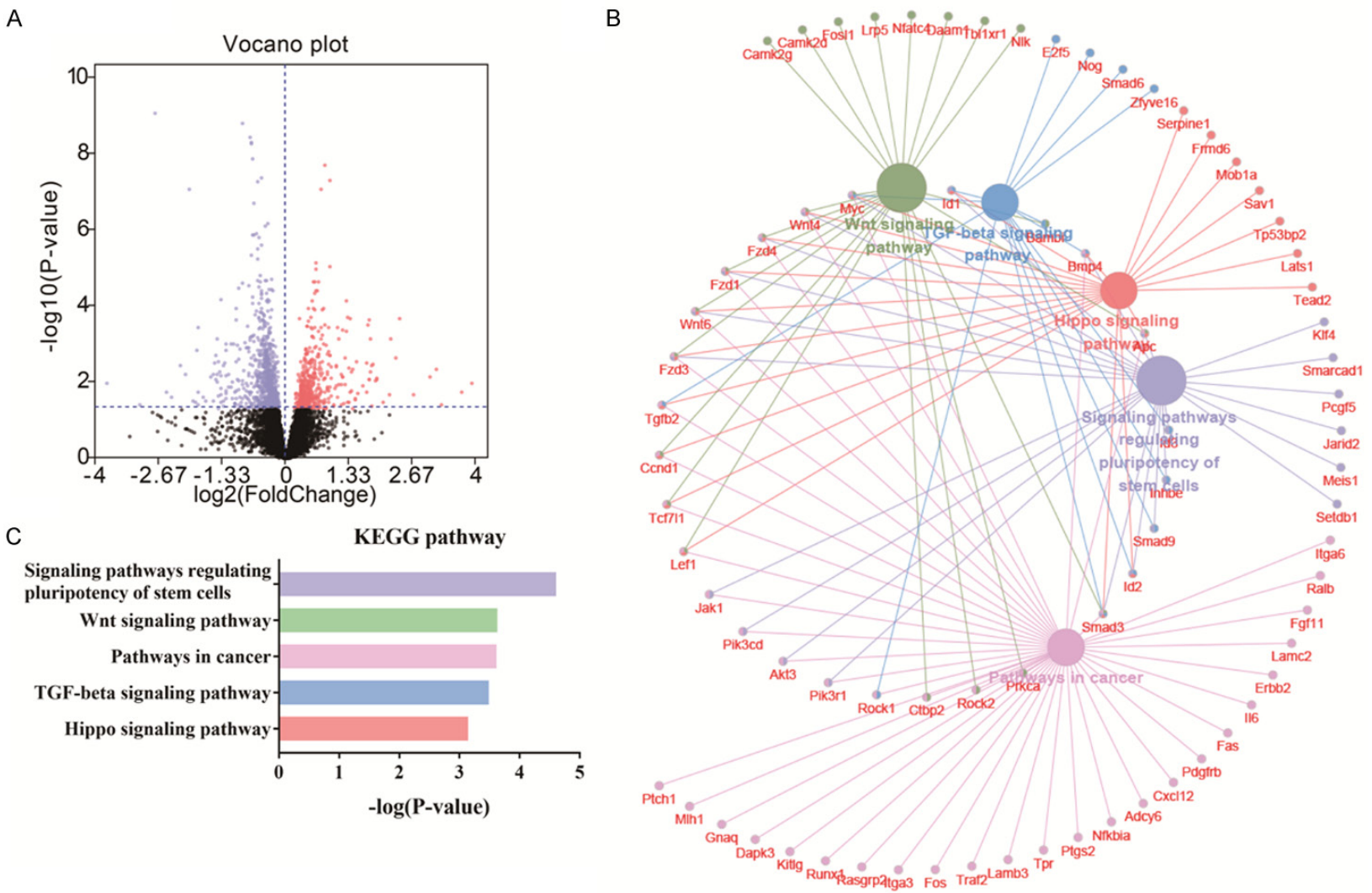

Figure 6. Transcriptomic analysis of H9c2 cells treated with APTBP. Hypoxic H9c2 cells were treated with APTBP (50 μM, 6 h) or left untreated. Then, total RNA was isolated for transcriptome analysis. A. Volcano plots showing the differentially regulated genes ($P<0.05$) after APTBP treatment. The volcano plot shows the log2 (fold change) on the x-axis against the -log10 (*P*-value) on the y-axis. B. The differentially regulated genes were then subjected to KEGG pathway enrichment analysis. The differentially regulated genes were analysed using the Cytoscape plug-in ClueGO + Cluepedia to identify statistically enriched KEGG pathways. C. The top five enriched KEGG pathways.

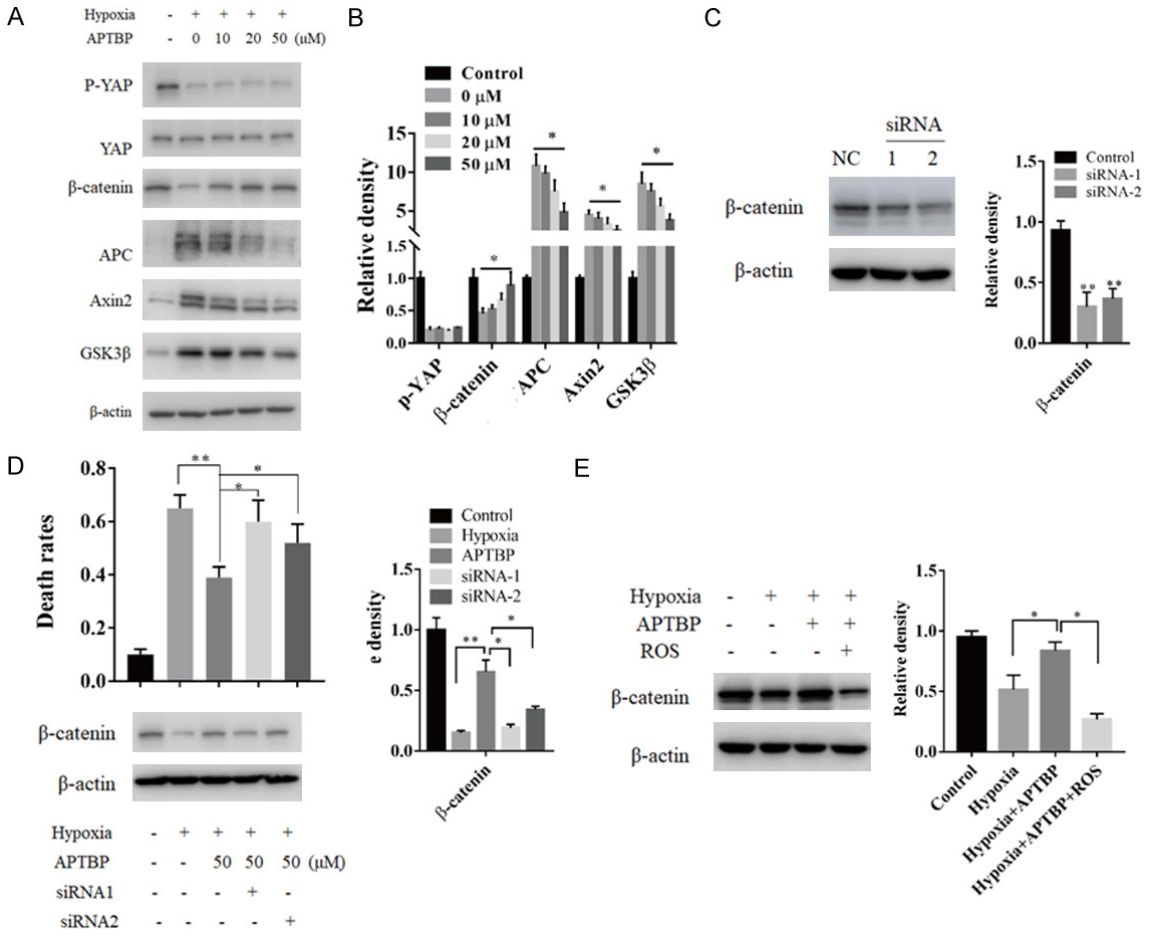

Figure 7. APTBP restored the activity of Wnt/β-catenin after hypoxic injury. A. H9c2 cells were pre-treated with APTBP for 1 h and then challenged with hypoxia (12 h)/reoxygenation (3 h). Then, the cells were harvested for Western blot analysis of β-catenin and its downstream target cyclin D1, phosphorylated YAP and the destruction complex, including APC, Axin2, and GSK3β. B. The relative density of the Western blot results. #P<0.05 versus the hypoxia group. The data from three replicate assays were collected and analysed. C. β-catenin knockdown efficiency of two siRNAs. **P<0.01 *P<0.05 versus the control group. D. After siRNA transfection of H9c2 cells for 48 h, the cells were treated as described and then the death rate was determined trypan blue analysis. E. Cells that underwent hypoxia (12 h)/reoxygenation (3 h) were pre-treated with APTBP (50 μM) combined with an ROS generator (0.5 Mm D-galactose + 0.015 U/ml GAO) for 1 h and then subjected to Western blotting. *P<0.05 versus the control group, ##P<0.01 versus the Hypoxia+APTBP group. Student's *t*-test was used to compare differences between groups. The data are shown as the means ± SD. All experiments were repeated three times with similar results.

results indicate no detectable effect of APTBP on the Hippo pathway.

Canonical Wnt signalling driven by β-catenin is an established, critical pathway in the cardiovascular system [18]. A previous study demonstrated that β-catenin overexpression decreased apoptosis in cardiomyocytes and cardiac fibroblasts and reduced I/R-induced damage [19]. These observations suggest a protective role of Wnt/β-catenin signalling in I/R and led us to hypothesise that APTBP protects cardiomyocytes against hypoxic stress through the Wnt/β-catenin signalling pathway.

Accordingly, we performed Western blotting to measure the activity of the Wnt/β-catenin signalling pathway. Hypoxic stress caused a significant decrease in the amounts of β-catenin and downstream cyclin D1, demonstrating an impairment of the Wnt/β-catenin signalling pathway (**Figure 7A**). In contrast, APTBP restored Wnt/β-catenin activity in a dose-dependent manner. The 50 μM APTBP-induced activity of β-catenin was equal to that of the control (**Figure 7A**, **7B**). β-catenin function is known to be abolished by a destruction complex composed of Axin2, adenomatous polyposis coli (APC), glycogen synthase kinase-3 beta (GS-

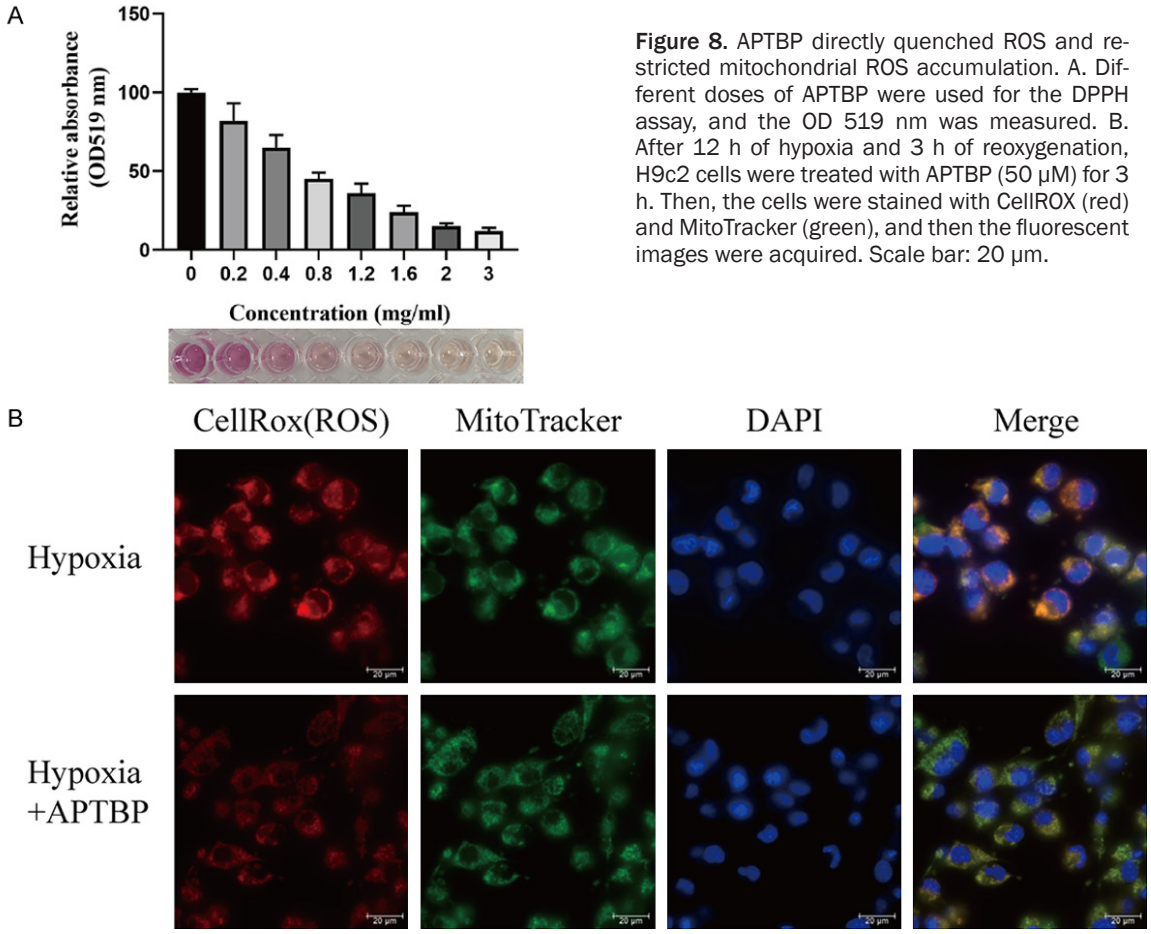

Figure 8. APTBP directly quenched ROS and restricted mitochondrial ROS accumulation. A. Different doses of APTBP were used for the DPPH assay, and the OD 519 nm was measured. B. After 12 h of hypoxia and 3 h of reoxygenation, H9c2 cells were treated with APTBP (50 μM) for 3 h. Then, the cells were stained with CellROX (red) and MitoTracker (green), and then the fluorescent images were acquired. Scale bar: 20 μm.

K3β) and casein kinase 1a (CK1a), which targets β-catenin for proteasomal destruction [20]. Consistently, the protein levels of APC and Axin2 were markedly elevated under hypoxic conditions, and APTBP administration repressed these levels in a dose-dependent manner (**Figure 7A**, **7B**). Moreover, the pattern of GS-K3β expression was similar to that of APC and Axin2, suggesting a coincident effect of APTBP on the negatively regulated complex. To confirm that the Wnt/β-catenin pathway is required for the cardioprotective effects of APTBP, we next examined the influence of β-catenin knockdown on APTBP functions. Two β-catenin siRNAs significantly reduced the levels of β-catenin, suggesting efficient inhibition of β-catenin signalling (**Figure 7C**). In the context of hypoxia, APTBP partially restored the protein level of β-catenin and reduced the H9C2 cell death rate to ~0.4, whereas silencing β-catenin increased the death rate to ~0.6 and ~0.5 (**Figure 7D**). Then, to determine whether APTBP restores Wnt/beta-catenin activity by scavenging ROS, we increased intracellular ROS levels by treating cardiomyocytes with D-galactose plus galactose oxidase (GAO) in the presence of APTBP. As shown in **Figure 7E**, the administration of D-galactose and GAO abolished the APTBP-restored expression of beta-catenin, suggesting that the APTBP-induced restoration of Wnt/β-catenin activity was dependent on ROS elimination. These results suggest that APTBP attenuates hypoxic damage in cardiomyocytes by restoring the hypoxia-induced impairment of Wnt/β-catenin signalling.

APTBP directly quenched ROS and restricted mitochondrial ROS accumulation

APTBP was regarded as an antioxidant when it was first identified. Thus, we examined its direct effect on ROS in vitro by performing a DPPH assay. The 2,2-diphenyl-1-picrylhydrazyl (DPPH) assay is routinely practised to assess the antiradical properties of different compounds. As shown in **Figure 8A**, APTBP significantly quenched ROS in vitro, suggesting a direct ROS scavenging function. In addition, we also mea-

sured mitochondrial ROS (MtROS), the major ROS source during I/R. Interestingly, MtROS increased under hypoxia/reoxygenation and was significantly decreased at 3 h after APTBP addition (**Figure 8B**), which was consistent with the time at which the peptide penetrated the cells (**Figure 1B**). Considering that the time was too short to initiate transcription and induce protein turnover, APTBP may possess direct antioxidant abilities and influence Wnt/β-catenin signalling by scavenging excessive ROS in the context of I/R.

Discussion

MI is a serious disease worldwide that has high morbidity and mortality. However, there is no effective approach to prevent myocardial reperfusion injury. Our present work revealed that APTBP, an antioxidant peptide, ameliorated myocardial ischaemia-reperfusion injury by restoring Wnt/β-catenin signalling activity.

ROS are well known as critical second messengers in various signalling pathways and are involved in different phases of the apoptotic pathway [21]. Our data suggest that APTBP reduces the levels of intracellular ROS, partly restores mitochondrial function and inhibits apoptosis. As an antioxidant, APTBP has been proven to inhibit lipid peroxidation and potently scavenge hydroxyl radicals, which are regarded as the strongest ROS [10]. However, those experiments were performed in an in vitro system, and the intracellular effect of APTBP on ROS generation was not clarified. In our study, APTBP decreased hypoxic stress-induced ROS accumulation in H9C2 cells and protected mitochondrial function, but whether APTBP functioned by scavenging ROS directly or by binding to and regulating specific proteins remains unclear.

A number of studies have documented that hydrogen peroxide (H_2O_2) induces a rapid increase in Wnt/β-catenin signalling that peaks approximately 20 min after stimulation, but this activity is reduced several hours later [22, 23]. Moreover, the administration of ROS scavengers such as superoxide dismutase (SOD) and catalase reduces β-catenin expression levels [24]. In our study, treatment with D-galactose plus GAO, which produces hydrogen peroxide in the medium that rapidly enters the cytosol, abolished the APTBP-induced restoration of β-catenin expression, suggesting that the APTBP-induced restoration of Wnt/β-catenin activity was dependent on its effect on ROS elimination. This observation indicates a dynamic response of Wnt/β-catenin signalling to ROS stimulation.

Recent studies have suggested that β-catenin can regulate cell survival, apoptosis and cardiomyocyte hypertrophy [25, 26]. In addition, β-catenin overexpression decreases apoptosis in cardiomyocytes and cardiac fibroblasts and reduces infarct size in rat models of I/R [19]. We showed that APTBP decreased apoptosis in association with an elevated level of β-catenin. This finding suggests that β-catenin activity is associated with hypoxia-induced cardiomyocyte apoptosis.

β-catenin function is well-known to be blocked by a destruction complex consisting of Axin2, APC, GSK3β and CK1a and that targets β-catenin for proteasomal destruction. Under the hypoxic conditions in our study, Wnt/β-catenin activity was significantly inhibited. We observed that the expression of APC and Axin2 was strongly elevated in response to hypoxia (**Figure 7D**, **7E**). These results indicate that the hypoxia-induced reduction in Wnt/β-catenin activity may contribute to the increased activity of the destruction complex. In addition, APC and Axin2 expression was decreased by treatment with APTBP, which suggests that APTBP function may be associated with the disruption of the destruction complex. However, whether and how ROS regulate Wnt/β-catenin activity in cardiomyocytes requires further investigation.

Although a valuable effect was observed in vitro, the in vivo effect was mild based on the evaluation of the myocardial infarction area and echocardiography. This result may be due to poor bioavailability at the target site. In addition, a sufficient dose and time were also required for high efficacy. In the future, the distribution of APTBP in various organs and modifications to improve peptide stability and specificity should be studied. In addition, in our present study, pre-treatment with APTBP was used in all experiments; however, the function of APTBP in cells exposed to hypoxia has not been determined. This issue needs to be addressed to evaluate the potential of APTBP in clinical therapy.

Taken together, our results suggest a cardioprotective role of APTBP in myocardial isch-

aemia-reperfusion injury. APTBP decreased ROS accumulation and cardiomyocyte apoptosis. The function of APTBP was associated with the restoration of hypoxia-induced impairments in Wnt/β-catenin signalling activity. Our study not only provides insights into the mechanisms underlying I/R but also presents novel opportunities for the design and development of more effective therapeutic strategies.

Acknowledgements

This study was supported by the Wuxi Establishment Site for Key Medical Disciplines (grant no. ZDXK12), the Medical Innovation Team of Jiangsu Province (grant no. CXTDB2017016), Wuxi Medical Development Discipline (grant no. FZXK001), National Natural Science Foundation of China (Grant no. 81901517), Jiangsu maternal and child health research project (Grant no. F201852), Wuxi Science and Technology Development Fund (Grant no. N20192039), Project of Wuxi health Commission (Grant no. M202003), Wuxi Young Medical Talents (grant no. QNRC094), the Wuxi Maternal and Child Health Research Project (grant no. FYKY201507), the Wuxi Health Bureau General Project (grant no. MS201401), the Nanjing Medical University General Programme (grant no. 2016NJMU125), the Young Project of the Wuxi Health and Family Planning Commission (grant nos. Q201815, Q201760, and Q201638), the Wuxi Hospital Management Centre Key Project (grant no. YGZXZ1513), and the Natural Science Foundation of Jiangsu Province of China (grant no. BK20151112).

Disclosure of conflict of interest

None.

Address correspondence to: Zhengying Li, Department of Neonatology, The Affiliated Wuxi Children's Hospital of Nanjing Medical University, Wuxi 214023, Jiangsu, China. E-mail: lizhy@njmu.edu.cn; Jian Zhou, Department of Pediatric Laboratory, The Affiliated Wuxi Children's Hospital of Nanjing Medical University, Wuxi 214023, Jiangsu, China. E-mail: jianzhou@njmu.edu.cn; Wei Qian, Department of Pediatrics, The Affiliated Wuxi Children's Hospital of Nanjing Medical University, Wuxi 214023, Jiangsu, China. E-mail: iamqianyizhou@163.com

References

[1] Eisenberg MS and Mengert TJ. Cardiac resuscitation. N Engl J Med 2001; 344: 1304.

[2] Mozaffarian D, Benjamin EJ, Go AS, Arnett DK, Blaha MJ, Cushman M, De FS, Fullerton HJ, Howard VJ and Huffman MD. Heart disease and stroke statistics-2015 update: a report from the American heart association. Circulation 2015; 131: e29.

[3] Yellon DM and Hausenloy DJ. Myocardial Reperfusion Injury. N Engl J Med 2007; 357: 1121-1135.

[4] Hess ML and Manson NH. Molecular oxygen: friend and foe. The role of the oxygen free radical system in the calcium paradox, the oxygen paradox and ischemia/reperfusion injury. J Mol Cell Cardiol 1984; 16: 969-985.

[5] Angelos MG, Kutala VK, Torres CA, He G, Stoner JD, Mohammad M and Kuppusamy P. Hypoxic reperfusion of the ischemic heart and oxygen radical generation. Am J Physiol Heart Circ Physiol 2006; 290: 341-347.

[6] Becker LB. New concepts in reactive oxygen species and cardiovascular reperfusion physiology. Cardiovasc Res 2004; 61: 461-470.

[7] Zhang Y and Ren J. Targeting autophagy for the therapeutic application of histone deacetylase inhibitors in ischemia/reperfusion heart injury. Circulation 2014; 129: 1088-1091.

[8] Khanna AK, Xu J and Mehra MR. Antioxidant N-acetyl cysteine reverses cigarette smoke-induced myocardial infarction by inhibiting inflammation and oxidative stress in a rat model. Lab Invest 2012; 92: 224.

[9] Ganesan B, Buddhan S, Anandan R, Sivakumar R and Anbinezhilan R. Antioxidant defense of betaine against isoprenaline-induced myocardial infarction in rats. Mol Biol Rep 2010; 37: 1319-1327.

[10] Je JY, Byun QHG and Kim SK. Purification and characterization of an antioxidant peptide obtained from tuna backbone protein by enzymatic hydrolysis. Process Biochem 2007; 42: 840-846.

[11] Wu RB, Wu CL, Liu D, Yang XH, Huang JF, Zhang J, Liao B, He HL and Li H. Overview of antioxidant peptides derived from marine resources: the sources, characteristic, purification, and evaluation methods. Appl Biochem Biotechnol 2015; 176: 1815-1833.

[12] Luo P, Dong G, Liu L and Zhou H. The long-term consumption of ginseng extract reduces the susceptibility of intermediate-aged hearts to acute ischemia reperfusion injury. PLoS One 2015; 10: e0144733.

[13] Li X. 2-Phenyl-4, 4, 5, 5-tetramethylimidazoline-1-oxyl 3-Oxide (PTIO•) Radical scavenging: a new and simple antioxidant assay in vitro. J Agric Food Chem 2017; 65: 6288-6297.

[14] Je JY, Qian ZJ, Byun HG and Kim SK. Purification and characterization of an antioxidant peptide obtained from tuna backbone protein by enzymatic hydrolysis. Process Biochem 2007; 42: 840-846.

[15] Barrera J. The Hippo signaling pathway coordinately regulates cell proliferation and apoptosis by inactivating Yorkie, the Drosophila Homolog of YAP. Cell 2005; 122: 421-434.
[16] Yu FX, Zhao B, Panupinthu N, Jewell JL, Lian I, Wang LH, Zhao J, Yuan H, Tumaneng K and Li H. Regulation of the hippo-YAP pathway by G-protein-coupled receptor signaling. Cell 2012; 150: 780-791.
[17] Zhao B, Ye X, Yu J, Li L, Li W, Li S, Yu J, Lin JD, Wang CY, Chinnaiyan AM, Lai ZC and Guan KL. TEAD mediates YAP-dependent gene induction and growth control. Genes Dev 2008; 22: 1962-1971.
[18] Caliceti C, Nigro P, Rizzo P and Ferrari R. ROS, Notch, and Wnt signaling pathways: crosstalk between three major regulators of cardiovascular biology. Biomed Res Int 2014; 2014: 318714.
[19] Hahn JY, Cho HJ, Bae JW, Yuk HS, Kim K, Park KW, Koo BK, Chae IH, Shin CS and Oh BH. β-catenin overexpression reduces myocardial infarct size through differential effects on cardiomyocytes and cardiac fibroblasts. J Biol Chem 2006; 281: 30979-30989.
[20] MacDonald BT, Tamai K and He X. Wnt/β-Catenin signaling: components, mechanisms, and diseases. Dev Cell 2009; 17: 9-26.
[21] Le BM, Clément MV, Pervaiz S and Brenner C. Reactive oxygen species and the mitochondrial signaling pathway of cell death. Histol Histopathol 2005; 20: 205.
[22] Funato Y, Michiue T, Asashima M and Miki H. The thioredoxin-related redox-regulating protein nucleoredoxin inhibits Wnt-beta-catenin signalling through dishevelled. Nat Cell Biol 2006; 8: 501.
[23] Shin SY, Kim CG, Jho EH, Rho MS, Kim YS, Kim YH and Lee YH. Hydrogen peroxide negatively modulates Wnt signaling through downregulation of beta-catenin. Cancer Lett 2004; 212: 225-231.
[24] Wang X, Mandal AK, Saito H, Pulliam JF, Lee EY, Ke ZJ, Lu J, Ding S, Li L and Shelton BJ. Arsenic and chromium in drinking water promote tumorigenesis in a mouse colitis-associated colorectal cancer model and the potential mechanism is ROS-mediated Wnt/β-catenin signaling pathway. Toxicol Appl Pharmacol 2012; 262: 11-21.
[25] Bergmann MW, Rechner C, Freund C, Baurand A, Jamali AE and Dietz R. Statins inhibit reoxygenation-induced cardiomyocyte apoptosis: role for glycogen synthase kinase 3β and transcription factor β-catenin. J Mol Cell Cardiol 2004; 37: 681.
[26] Antos CL, McKinsey TA, Frey N, Kutschke W, McAnally J, Shelton JM, Richardson JA, Hill JA and Olson EN. Activated glycogen synthase-3β suppresses cardiac hypertrophy in vivo. Proc Natl Acad Sci U S A 2002; 99: 907-912.

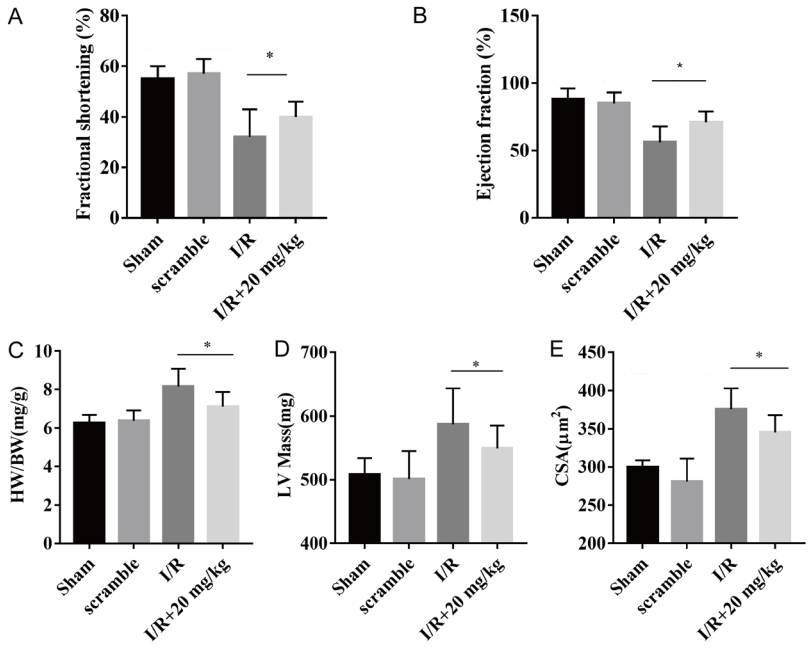

Figure S1. APTBP attenuated I/R-induced impairment of myocardial function. After the I/R procedure, the rats were subjected to echocardiography analysis, and the related indices were measured. A. Fractional shortening. B. Ejection fraction. C. HW/BW ratio. D. LV mass. E. Relative cardiomyocyte CSA. Student's *t*-test was used to compare differences between groups. The data are shown as the means ± SD. Each group contained 6 rats.

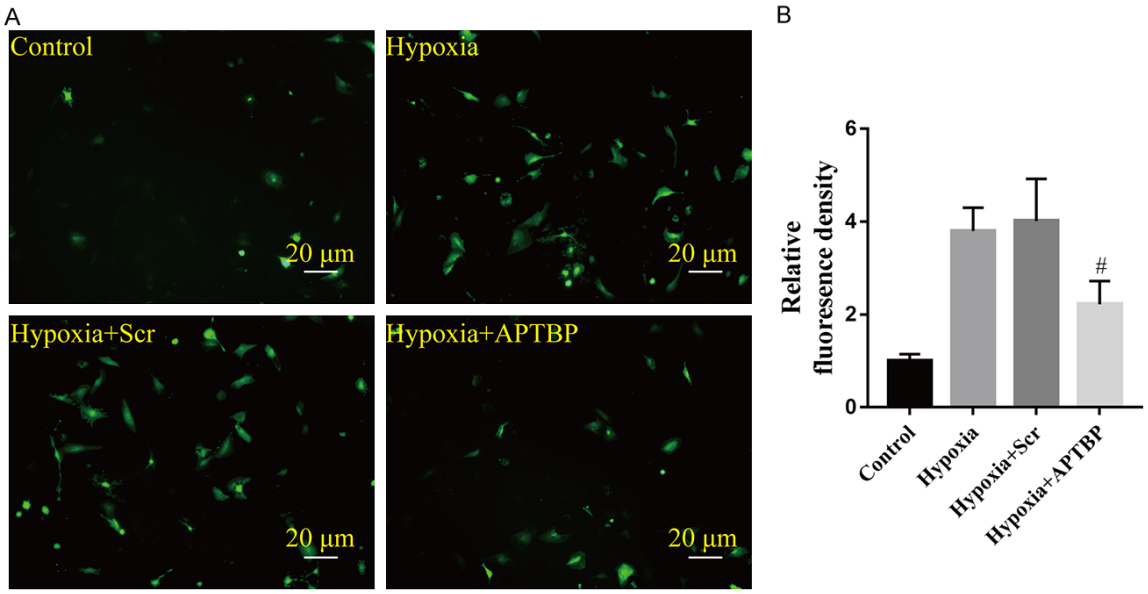

Figure S2. APTBP diminished hypoxia-induced ROS accumulation in primary rat cardiomyocytes. Primary cardiomyocytes were pre-treated with APTBP (50 μM) for 1 h and then challenged with 12 h of hypoxia and 3 h of reoxygenation. Intracellular ROS levels were then measured using DCFH-DA. A. Representative images of ROS staining; scale bar: 20 μm. B. The relative fluorescence intensity. $^{\#}P<0.05$ versus the I/R group. Student's *t*-test was used to compare differences between groups. The data are shown as the means ± SD. The experiment was repeated three times with similar results.